REPORT DOCUMENTATION PAGE

Form Approved
OMB No. 0704-0188

1. REPORT DATE *(DD-MM-YYYY)*	2. REPORT TYPE	3. DATES COVERED *(From - To)*
08-03-2011	Journal Article	

4. TITLE AND SUBTITLE

Comparison of electrostatic fins with piezoelectric impact hammer techniques to extend impulse calibration range of a torsional thrust stand (Preprint)

5a. CONTRACT NUMBER

5b. GRANT NUMBER

5c. PROGRAM ELEMENT NUMBER

6. AUTHOR(S)
Anthony P. Pancotti (ERC), Martin S. Hilario, and Matthew Gilpin (Univ of Southern California)

5d. PROJECT NUMBER

5f. WORK UNIT NUMBER
50260542

7. PERFORMING ORGANIZATION NAME(S) AND ADDRESS(ES)

ERC Inc
10 E. Saturn Blvd.
Edwards AFB, CA 93524, USA

University of Southern California
Dept. of Mechanical and Aerospace Engineering
Los Angeles, CA 90089

8. PERFORMING ORGANIZATION REPORT NUMBER

AFRL-RZ-ED-JA-2011-075

9. SPONSORING / MONITORING AGENCY NAME(S) AND ADDRESS(ES)

Air Force Research Laboratory (AFMC)
AFRL/RZS
5 Pollux Drive
Edwards AFB CA 93524-7048

10. SPONSOR/MONITOR'S ACRONYM(S)

11. SPONSOR/MONITOR'S NUMBER(S)
AFRL-RZ-ED-JA-2011-075

12. DISTRIBUTION / AVAILABILITY STATEMENT

Distribution A: Approved for public release; distribution unlimited (PA #10908).

13. SUPPLEMENTARY NOTES
For publication in American Institute of Physics: Review of Scientific Instruments, April 2011

14. ABSTRACT

With growing interest and development of large pulsed plasma electric propulsion devices, it has become necessary to accurately measure their thruster performance (1). Direct thrust measurements are the best way to measure the impulse of a propulsion device which requires it to be mounted entirely on the thrust stand. In many cases this means the thrust stand must support 10 to 100's of kilograms and still be able to resolve *m*Ns worth of impulse. With the development of this new class of thrust stand, an accurate and repeatable method of calibration is needed. Two such calibration methods have been examined and compared. Electrostatic fin (ESF) and piezoelectric impact hammer (PIH) calibration systems were simultaneously tested on a large scale torsional thrust stand system. The use of these two methods allowed the stand to be calibrated over four orders of magnitude, from 0.01*m*Ns to 750*m*Ns. The ESF system produced linear results within 0.52% from 0.01*m*Ns to 12*m*Ns, while the PIH system extended this calibration range from 1*m*Ns to 750*m*Ns with an error of 0.99%. These two calibration methods also agreed within 4.51% over their overlapping range of 10 to 20 *m*Ns.

15. SUBJECT TERMS

16. SECURITY CLASSIFICATION OF:			17. LIMITATION OF ABSTRACT	18. NUMBER OF PAGES	19a. NAME OF RESPONSIBLE PERSON
					Mr. Marcus Young
a. REPORT	b. ABSTRACT	c. THIS PAGE			19b. TELEPHONE NUMBER *(include area code)*
Unclassified	**Unclassified**	**Unclassified**	SAR	9	N/A

Comparison of electrostatic fins with piezoelectric impact hammer techniques to extend impulse calibration range of a torsional thrust stand

Anthony P. Pancotti,[1, a)] Martin S. Hilario,[2, b)] and Matthew Gilpin[2, c)]
[1)] *ERC Inc, Edwards Air Force Base, CA 93524*
[2)] *University of Southern California, Department of Mechanical and Aerospace Engineering, Los Angeles, CA 90089*

(Dated: 23 March 2011)

With growing interest and development of large pulsed plasma electric propulsion devices, it has become necessary to accurately measure their thruster performance[1]. Direct thrust measurements are the best way to measure the impulse of a propulsion device which requires it to be mounted entirely on the thrust stand. In many cases this means the thrust stand must support 10 to 100's of kilograms and still be able to resolve mNs worth of impulse. With the development of this new class of thrust stand, an accurate and repeatable method of calibration is needed. Two such calibration methods have been examined and compared. Electrostatic fin (ESF) and piezoelectric impact hammer (PIH) calibration systems were simultaneously tested on a large scale torsional thrust stand system. The use of the these two methods allowed the stand to be calibrated over four orders of magnitude, from $0.01mNs$ to $750mNs$. The ESF system produced linear results within 0.52% from $0.01mNs$ to $12mNs$, while the PIH system extended this calibration range from $1mNs$ to $750mNs$ with an error of 0.99%. These two calibration methods also agreed within 4.51% over their overlapping range of 10 to 20 mNs.

I. INTRODUCTION

Thrust diagnostics for electric propulsion devices typically require the measurement of very small impulses or steady state forces. Because of this, a number of different methods have been used for accurate and repeatable calibration of thrust stands in the nN to mN range. These techniques include gas dynamic calibration[2], swinging known masses[3,4], electrostatic combs[5], impact pendulums[6], and impact hammers[7].

Selden *et al.*[8] performed a comparison of electrostatic combs (ESC) and gas dynamic (GD) calibration systems. ESC and GD calibration were found to agree to within 8% for force levels between $35nN$ to $1\mu N$. ESC calibration systems have been in implemented in a number of small impulse measurements and have proven to be reliable and accurate over four orders of magnitude, from 10's of nNs[9] to $100\mu Ns$[10]. In practice however, a single ESC system is only applicable over a range of two orders of magnitude and geometric requirements limit the practical max impulse to $1mNs$. The newly developed Piezoelectric Impact Hammer (PIH) calibration system overcomes geometric limits of ESC calibration systems and can impart maximum impulses has high as 100's of mNs as required for the direct testing of new pulsed plasma electric propulsion devices[1].

In this work an ESC and PIH calibration system are combined in order to calibrate over four orders of magnitude. Specifically the ESC and PIH calibration are compared in the range in which they overlap. Both calibration methods, which rely on different physical principles, are validated against one another, verifying that each individual method is an accurate method for thrust stand calibration.

II. ELECTROSTATIC CALIBRATION SYSTEM

The first calibration system tested was an electrostatic system. Electrostatic systems are advantageous because they can be used at atmosphere or under full vacuum and are capable of applying very small forces in a repeatable and accurate manner. They have already been compared with a gas dynamic system, with reasonable agreement, and have been used extensively to calibrate a number of nano-newton thrust stands[11–15]

There are however several problems with electrostatic calibration methods. Conventional electrostatic plate systems produce a force that is inversely proportional to the square of the gap distance. This can often be problematic as one of the calibration plates is attached to the thrust stand and moves with respect to the fixed plate as the stand oscillates. The electrostatic fin (ESF) design eliminates the gap distance dependency and shows very constant electrostatic forces for a significant range of gap distances[8]. Additionally the scaling and validation of large linear fin systems have been addressed.

A. Fin Design

The electrostatic comb design as described by Selden *et al.* used precise geometry to compare experimental results with theoretical applied forces predicted by Johnson and Warne[16]. However, this comparative work required

[a)] anthony.pancotti.ctr@edwards.af.mil; AFRL/RZSA/Advanced Concepts Group, 10 E. Saturn Blvd, Edwards Air Force Base, CA 93524
[b)] Air Force Co-op, Edwards Air Force Base, CA 93524
[c)] ERC Co-op, Edwards Air Force Base, CA 93524

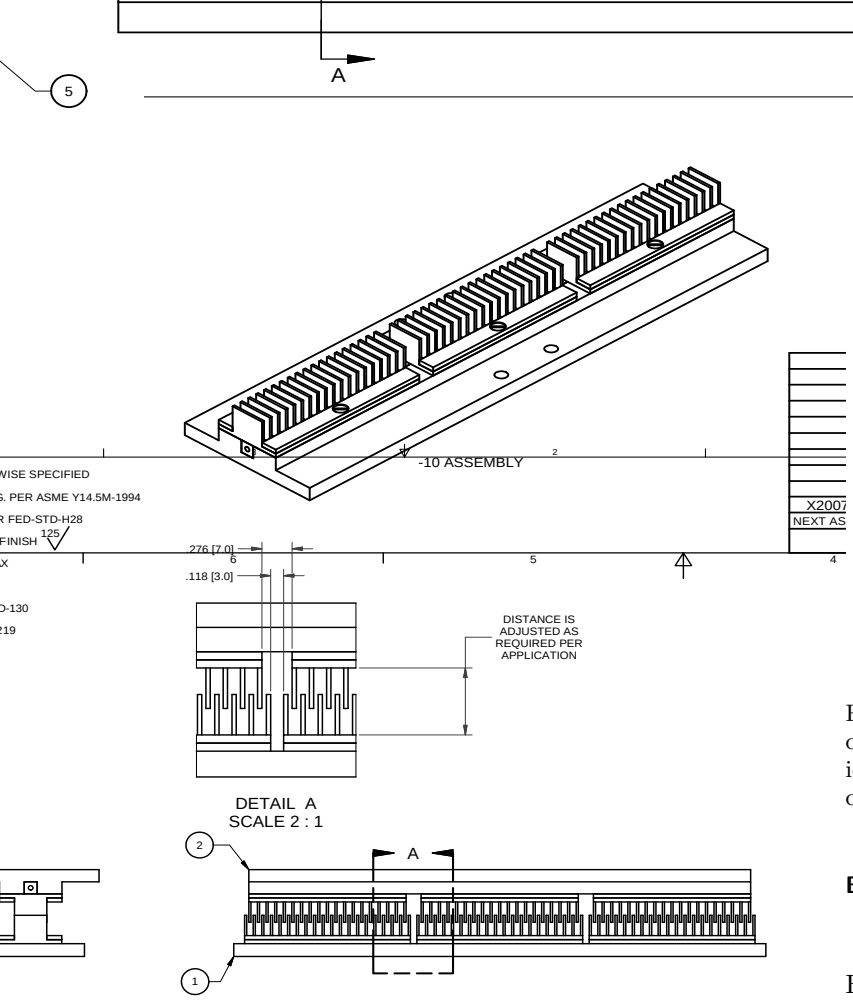

FIG. 1. Diagram of the Electrostatic Fin system utilized for calibration comparison

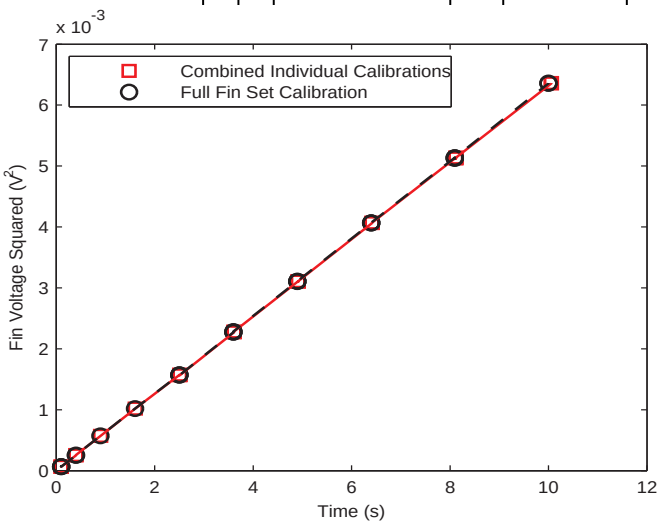

FIG. 2. Calibration sets for individual and combined scale calibration methods. Both sets are virtually identical, validating the individual method as well as initial calibration curves

impulses larger than those available from Selden's symmetric comb system. Thus, the electrostatic comb design has been scaled up by modifying the symmetric comb, extending it into a long fin. Three sets of these Electrostatic Fins (ESF) were mounted in a row to impart even more force to the the stand. Figure 1 shows the fin assembly geometry. Note that the grounded set of combs contains one more fin in order to fully isolate each group of fins and limit interaction between the sets.

In order to quantify the applied force from the ESF sets, they were initially calibrated using a micro-balance. The three fin sets were calibrated individually, by placing one grounded fin group on the scale and the corresponding charged fin group above. Voltages were applied and the corresponding forces were recorded. This data was then compared to a scale calibration utilizing all three sets simultaneously in their end configuration. Figure 2 shows the results of both calibrations. The results of the combined micro-balance calibration were within 1% of the calibration curve produced by treating each fin set individually, thus validating the use of ESF arrays. The fins were also tested for their independence to fin engagement, and produced a constant force for engagement over a range of 2 mm which is in agreement with Selden[8].

B. Electrostatic Fin Voltage Overshoot

During the course of testing it became apparent that ESF voltage values were higher than the voltage specified for a given test. The voltage error when propagated produced an overall error of 1% in the final calibration curve. Initial investigation revealed a voltage spike when the fins were energized on the order of two percent of the steady state voltage during a pulse. An example of this can be seen in Figure 3. When this pulse was sampled at a higher sampling rate (10,000 Hz), it was determined that the initial voltage spike was an aliased reading of a sinusoidal voltage oscillation. This phenomena has not been previously mentioned in literature concerning the operation of an ESF system.

The sinusoidal oscillation of the voltage on the electrostatic fins was analogous to the behavior of an underdamped second order system in response to a step input. Measuring the electrostatic fins revealed a capacitance of approximately 100 pF at a 3 mm engagement. This capacitance causes the fins to behave as part of an LRC circuit which results in voltage oscillations. By adding a resistor in series between the pulse generator and the electrostatic fins the damping coefficient was increased and voltage oscillations were reduced dramatically. Figure 4 shows the effects of a series resistor as well as the effects of no loading on the pulse generator.

III. PIEZOELECTRIC IMPACT HAMMER SYSTEM

The second calibration method tested was a Piezoelectric Impact Hammer (PIH) System. This calibration system was developed utilizing off-the-shelf piezoelectric

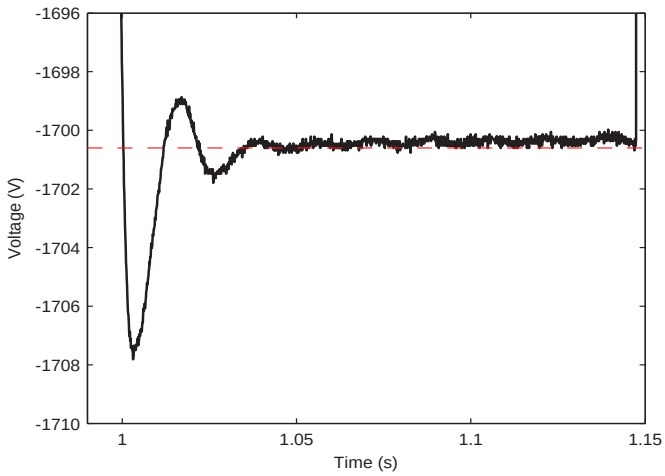

FIG. 3. Example of the initial voltage spike present in electrostatic fin calibration pulses. Average pulse voltage is shown in red.

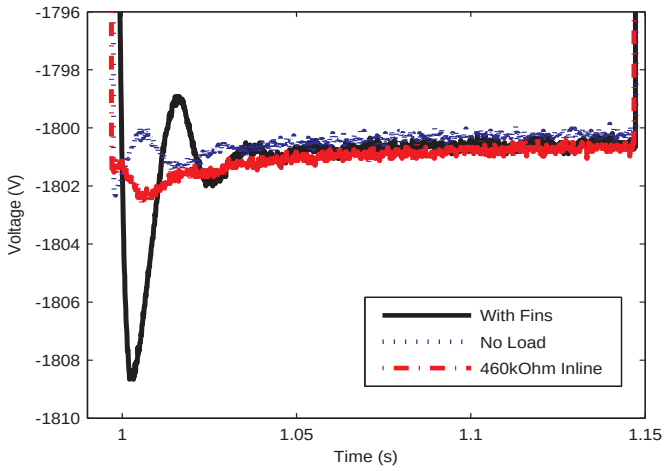

FIG. 4. Effects of different loads on pulsed voltage overshoot. Placing a resistor in series with the electrostatic fins damps oscillations due to the capacitive effected of the fins.

components and mechanisms were developed to mount and actuate the hammer in repeatable fashion. Additionally, the factory calibration of the hammer was verified in house.

A. Hammer Mechanism Design

The PIH calibration system utilized a PCB 086C02 piezoelectric impact hammer. A rotation shaft was clamped to the hammer's approximate center of mass and supported by dual ball bearings. The hammer was rotated about this pivot point using a servo motor attached by a thin control arm near the end of the hammer's handle. Figure 5 show the basic mechanical setup of the PIH system.

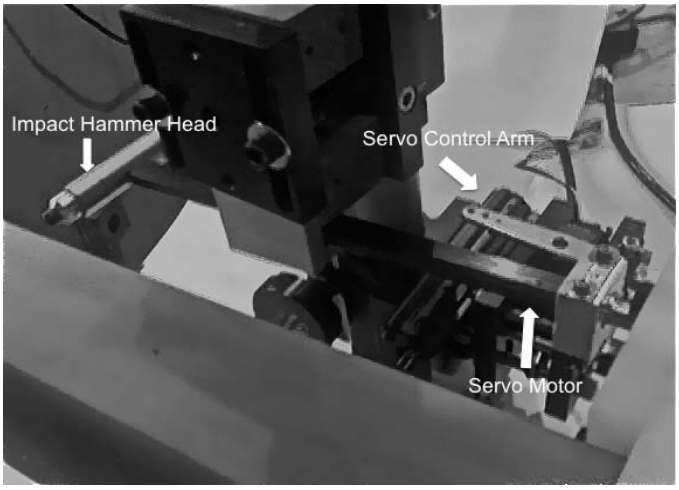

FIG. 5. Photograph of the hammer, pivot bearings, and control servo set up in orientation to the thruststand

The impact hammer head, as shown in Figure 5, was rotated counterclockwise by the servo linkage which was capable of position, velocity and acceleration control. When the hammerhead strikes the thrust stand, the polyurethane tip initiates the hammer rebound and the original position is then restored by returning the actuator to the original position. Accurate position control and fast actuator response time is necessary to provide a consistent impact magnitude and prevent double or multiple taps.

Based on these requirements, the Futaba model BLS-155 was selected to control the impact hammer. This servo unit contains metal gearing to reduce backlash and gear slop, contains an onboard processor to improve position and control velocity accuracy, and the constant level of torque necessary to provide the rotational force to drive the hammer. Through pulse width modulation control, the Futaba servo could be accurately controlled through a full 120 degree range and be accurately brought back to a neutral position after initiating a hammer strike.

B. Impact Hammer In-House Calibration

The impact hammer was calibrated in house to validate experimental use in the time domain as the PCB 086C02 was primarily developed for frequency response testing and frequency domain analysis. The calibration system consisted of a freely suspended reference mass with an attached accelerometer. The force experienced by this mass during a hammer strike is the reference mass multiplied by the acceleration value from the calibrated accelerometer. The resulting force can then be matched to the impact hammer voltage output. Dividing the peak output

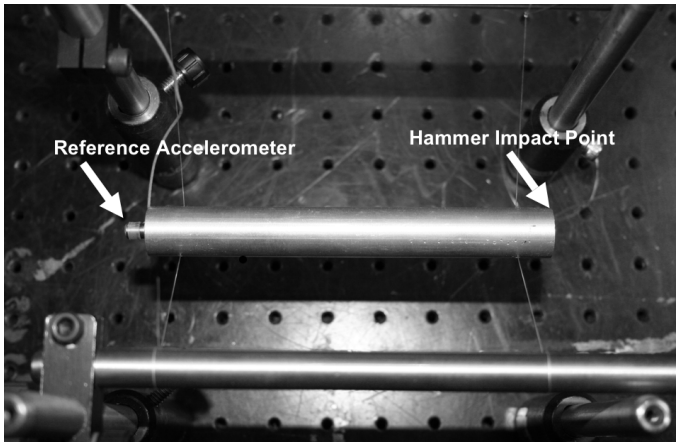

FIG. 6. Photograph of the reference weight system used to calibrate the impact hammer. The weight is suspended on two sides by low weight nylon line and is allowed to oscillate freely along a single axis. This system is analogous to the system used by PCB for in house calibrations.

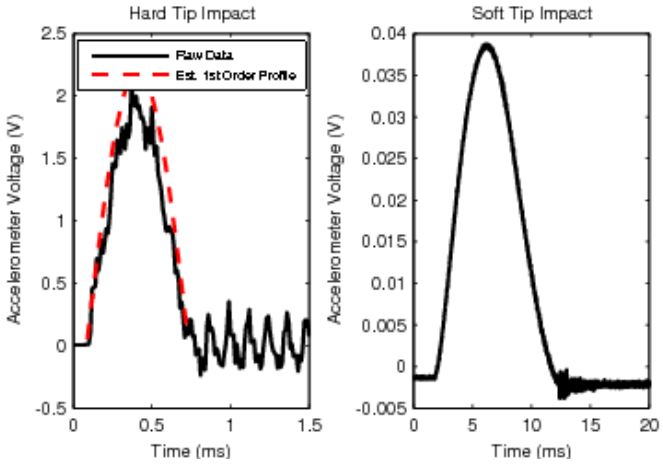

FIG. 7. Comparison of acceleration profiles produced with medium plastic and soft rubber hammer tips.

signal of the impact hammer by the peak force yields a value for hammer sensitivity in mV/N for a given strike.

Initial calibration attempts were made with the medium plastic impact cap, however, the results obtained were unreliable. Striking the reference mass with this relatively hard tip produced audible acoustic ringing and the resulting vibrations were measured by the accelerometer. Accelerometer data contained multiple higher order oscillations which can be seen in Figure 7 that undercut the peak values for acceleration. As a result, in house calibration using the medium plastic impact cap was approximately 10% lower than the factory calibration certification for the impact hammer.

A second calibration attempt was made with the soft rubber impact cap to eliminate the effects of acoustic ringing in the reference mass. The soft tip impacts yielded lower peak acceleration values and resulted in longer strike times, however, higher order oscillations were removed from the data. The sample soft tip impact accelerometer output in Fig. 7 shows the resulting smooth profile with a clearly defined peak acceleration. These profiles were well suited to the time domain hammer calibration and required the use of the soft impact tip throughout all system testing. The calibration of over 50 soft tip impacts were averaged to determine a hammer sensitivity value of $12.50 mV/N$ which is within 1% of the factory calibration value. This agreement confirmed proper operation of the impact hammer as well as the collection and analysis method used.

C. Impact Hammer Servo Control

Accurate control and automation of the impact hammer is critical to elimination of multiple hammer strikes. Moreover, a repeatable impulse requires known and precise positioning of the thrust stand strike point to generate a desired impulse width and amplitude.

The fast-response of the chosen servomotor combined with software control, which actively corrected for capacitor drift errors, allowed precise knowledge of the hammer position. By controlling the hammer with this method, it was possible to generate known and repeatable small impulses for purposes of comparison with the ESF systems.

Two methods of generating impulses include (1) rapid strikes that return the hammer after elastic impact for smaller impulses and (2) forcing the length of the hammer impact through servo control for larger impulses. For small single strikes that return based on the elasticity of the hammer tip, impulse is modulated by changing the velocity of the hammer as it strikes the stand. This method allows for impulses up to 200 mNs, with a pulse width of $1ms$.

Larger impulses were obtained by altering the impact duration between the hammer and the stand. Longer impact lengths were obtained by using servo control to force contact past elastic rebound. The hammer was programmed to rotate through a given range and the offset distance between the hammer tip and the strike point was adjusted. By decreasing the offset distance, a larger part of the rotation range was in the path of the stand, and a long duration higher impulse strike would result. Similarly increasing the offset distance resulted in a lower impulse. This method resulted in a linear relationship between offset distance and impulse for a given strike. As the total pulse times for small and large impulse methods occur within one-tenth of the period of the thrust stand, integrating the force over time resulted in the same deflections based on the total impulse.

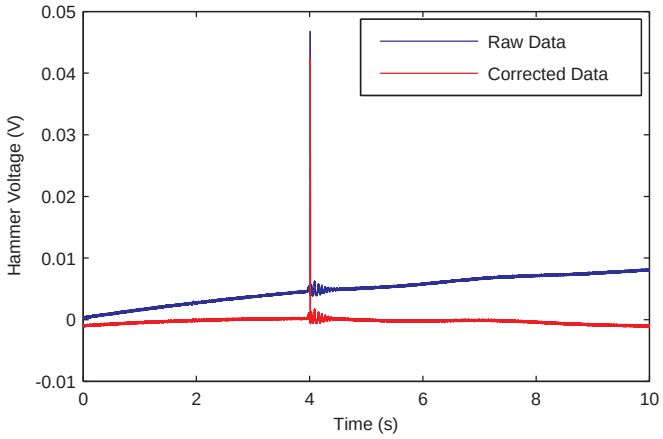

FIG. 8. Raw and corrected impact hammer force profiles produced from sample thrust stand impact.

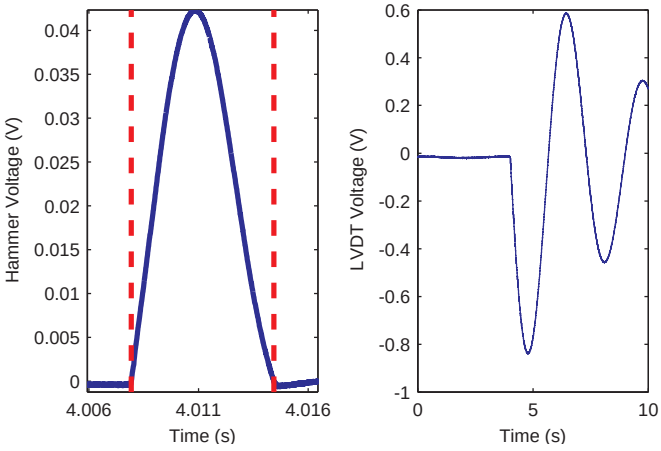

FIG. 9. Impact hammer force profile and resulting LVDT deflection data from the sample hammer strike in Fig. 8 .

D. Impact Hammer Data Correction and Analysis Methods

All data collected from the impact hammer was processed to correct for non-zero offset as well as a voltage drift slope present in the data acquisition system. In order to obtain a value of total hammer impulse for a strike, it is essential to level and zero the instantaneous force profile collected before numeric integration. Figure 8 shows raw and corrected impact hammer data for a sample strike. There is approximately $1mV/s$ drift as well as a non-zero voltage offset. The raw data is leveled and zeroed to produce a corrected trace. These same data correction routines were also used during the in-house calibration of the impact hammer. The result from the analysis of corrected data resulted in a less than 1% deviation in linearity between peak hammer voltage and peak accelerometer voltage.

Once corrected, data is scanned for the hammer impact ignoring secondary oscillations induced by both servo motion of the hammer and vibration of the hammer assembly after making contact with the stand. An example of this isolated hammer impact is shown in Figure 9, along with the resulting thrust stand deflection. This figure shows properly prepared data for numerical integration. The hammer impact data is then numerically integrated, and multiplied by the hammer sensitivity factor to produce a value for total impulse delivered. The integration bound requirements are standardized for all tests to ensure that similar sections of the hammer profile are integrated for all testing.

IV. EXPERIMENTAL SETUP AND PROCEDURE

The ESF and PIH calibration systems were both set up on a high impulse torsional thrust stand. The stand consisted of a 4 ft long 1.5 in by 3 in solid G10 beam. In addition, the support structure was also manufactured from G10 in order to provide a rigid, yet nonconductive thrust stand preventing interference with pulsed inductive thrusters. The beam rotates about 2 flexure pivots that provide frictionless motion and the restoring force. The oscillations are damped utilizing eddy currents created by a stand-mounted copper plate traversing a magnetic field created with stationary neodymium magnets. 30 kg blocks with a total moment of inertia of 9.50 kgm^2 were added and 1.00-inch spring flexures were selected, giving the stand a period of 8 s and a max deflection of 2 mm from a 500 mNs impulse.

The deflection of the stand was measured by a Linearly Variable Differential Transformer (LVDT). The PR-812-050 model that was used has a nonlinearity error of 0.25% FSO in the measurement range of ± 1.5 mm. This range corresponds to output voltage of ± 3.75 V. For the full range testing using the hammer, the stand deflected outside the recommend range to output voltages of ± 10 V. The linearity over this range was determined to be 0.5% FSO which is still within performance required for testing.

The ESF and PIH were calibrated with methods specified in Section II A and Section III B before they were installed on the thrust stand. The thrust stand and calibration systems were tested under vacuum condition of $2 \times 10^{-5} torr$. The location of the force generation for both calibration methods was at the same distance from the center of rotation and the PIH system was tested against the common 3 mm ESF engagement. For all testing, the range of the initial thrust stand oscillation was considered to be the stand displacement for a given impulse.

It is also important to note that systemic voltage offsets, channel cross-talk at high sampling rates, and accurate voltage calibrations must be considered when taking simultaneous thrust stand calibration measurements. Since multiple charge-coupled devices are being used si-

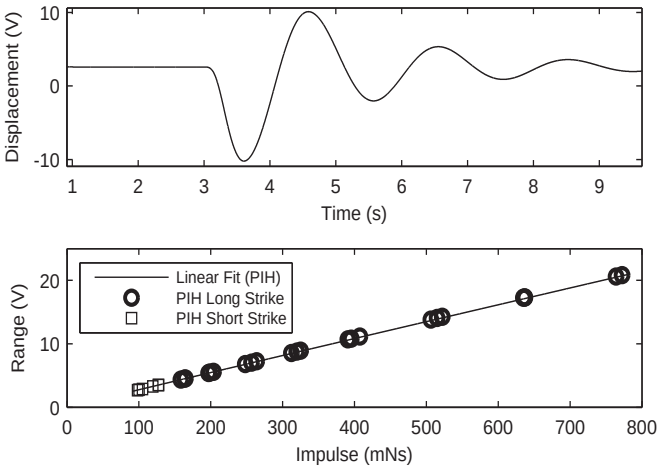

FIG. 10. Data sample from PIH calibration system. (Top) Resultant stand oscillations for the maximum measurable hammer strike of 750 mNs. (Bottom) Displacement range from impulses applied from PIH calibration.

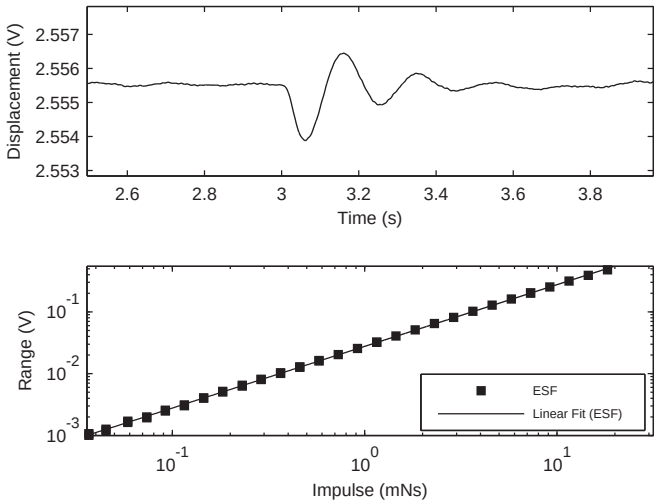

FIG. 11. Data sample from ESF calibration system. (Top) Resultant stand oscillations for the minimum resolvable electrostatic fin impulse of $0.01mNs$. (Bottom) Displacement range from impulses applied from ESF calibration.

multaneously, care must be taken to avoid interference. To ensure reliable data, all experimental channels were sampled utilizing independent ADCs.

V. RESULTS AND DISCUSSION

The PIH is a desirable calibration method for large impulses on a torsional thrust stand. The servo control system allowed the hammer to precisely and repeatably strike the stand with impulses ranging from 0.5 to 600 mNs. The maximum possible impulse was limited by the LVDT displacement range of 3 mm. However, placing the LVDT closer to the pivot point along the thrust stand arm can increase the impulse range without exceeding the maximum LVDT displacement range at the cost of small impulse fidelity. Figure 10 shows a 500 mNs impulse imparted to the stand resulting in a deflection of 12 V or a physical displacement 2.1 mm. As mentioned in Section III C, two methods were used to impart impulse to the stand through fine control of the servo motor. At around 140 mNs, the impulse switched from a single tap to a push mode of operation. As can be seen in Figure 10, there is no discontinuity between these two methods. The Long Strike method agrees with the calibration line of the Short Strike to with in 0.5%

In contrast, the ESF system is designed for generating very small impulses. The lower limit of this impulse is a function of the noise in a given LVDT and data acquisition system. Very small thrust stand oscillations are subject to disturbances, either electrical or vibrational, which can drown out the signal from a small impulse. Typically a minimum signal to noise ratio of 20 is needed to accurately resolve displacement. Figure 11 shows the displacement in terms of LVDT voltage for a 0.1 mNs impulse. Since only the initial oscillation of the stand is considered, the impulse can still be resolved despite the high level of signal noise. Figure 11 shows the results of a low impulse calibration using the ESF resulting in a linearity of approximately 1 %.

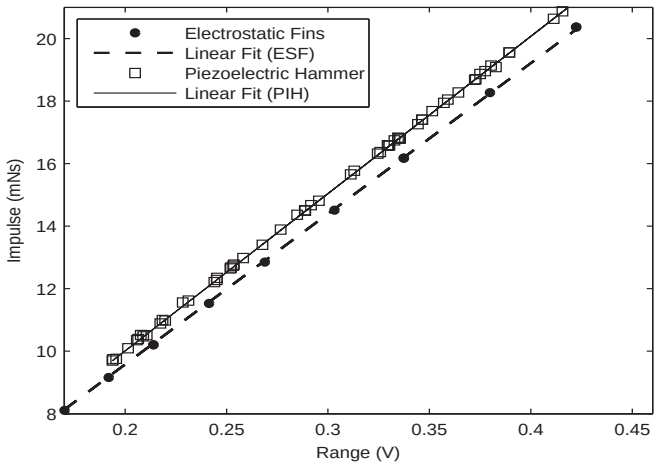

FIG. 12. Comparison of ESF and PIH in the impulse region where the two systems overlap

The ESF and PIH calibration systems were compared over an impulse range from 10 to 20 mNs; 10 mNs being the smallest force achievable from the PIH and 20 mNs the largest force achievable from the ESF. Figure 12 shows LVDT displacement in volts as a function of the applied impulse over this entire range. ESF data in this range is very linear with a percent deviation of only 0.33%. The PIH within this range is also very con-

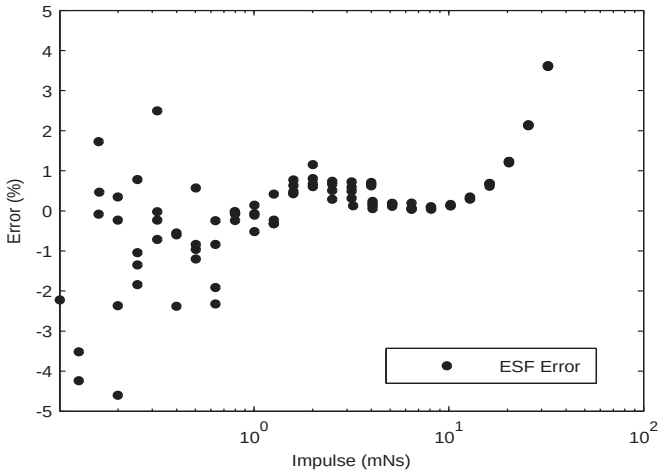

FIG. 13. Error dispersion across the full range of the ESF system

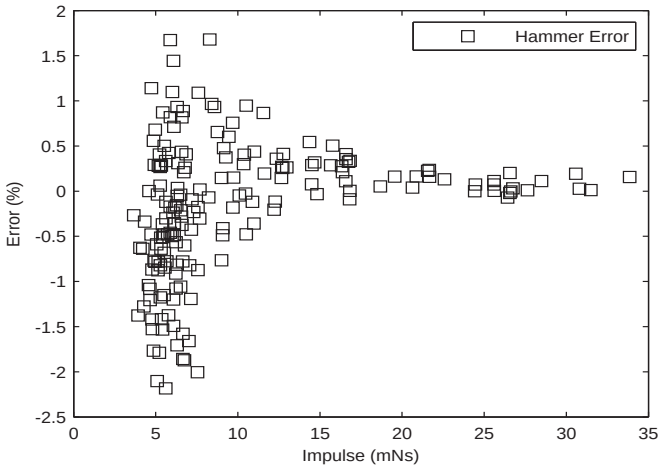

FIG. 14. Error dispersion across the full range of the PIH system

sistent and linear and has an average percent divination of 0.31%. Across the combined four orders of magnitude range, the PIH and ESF agree within 4.5 %.

Looking closely at the errors associated with both calibration methods, it is much easier to see the limitations of the two systems. Figure 13 shows the percent deviation from the linear fit through the entire range of ESF data. At low impulse levels, accuracy decreases and signal-to-noise issues become more prevalent. At larger impulse levels, the strike time becomes more significant with respect to the thrust stand period. As the impulse time approaches $1/10^{th}$ the period of the stand, the error increases to 1% as discovered earlier by D'souza and Ketsdever[9].

A similar error trend for the PIH is displayed in Figure 14. At low impulses, the zero location and numerical integration error of the instantaneous force profile decreases accuracy. This effect along with decreased repeatability inherent in small hammer strikes causes symmetric dispersion of the error. At higher impulse ranges these errors in the PIH become less prevalent resulting in the increased linearity.

Figure 15 plots LVDT deflection in volts as a function of applied impulse over the full combined range of both systems. Combining the calibration systems, it is possible to accurately calibrate a system over approximately 6 orders of magnitude from $0.01mNs$ to 750 mNs. The calibration line fitted in Figure 15 includes calibration points from both systems and results in an overall error of 0.5 % across the range. This indicates a strong agreement between the ESF and PIH calibration systems. Additionally, the coherence of calibration points based upon systems utilizing different physical principles and data collection methods validates both systems.

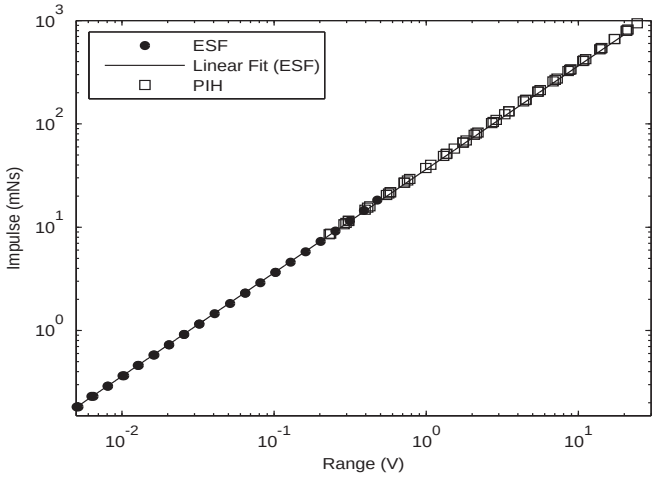

FIG. 15. Calibration testing shows maximum deflection to be linearly dependent on the delivered impulse as calculated with current impulse hammer techniques. Impulses are consistent to within 0.5% average error.

VI. CONCLUSION

The measurements and techniques investigated in this work have broadened the calibration options available to thrust stand designers and operators. The Piezoelectric Impact Hammer (PIH) system offers a new calibration technique for small impulse thrust stands and is accurate over a larger impulse range than other available methods. Through precise servo control of the piezoelectric hammer, the PIH calibration method is repeatable, accurate, and functional over a range from 1 to 1000 mNs of impulse. The PIH system offers a highly accurate option for thrust stand calibration without the precise machining demanded of the ESFs and the maximum impulse

limitations imposed by ESF geometry.

The PIH system has been validated experimentally against an Electrostatic Fin System (EFS) derived from previous electrostatic calibration work[8]. The two systems agreed to within 4.5 % within the region of overlap and within 0.5 % across the combined range of both systems. By referencing and refining the well established electrostatic calibration method, the PIH can produce calibration results with a great level of confidence. In addition, the EFS calibration system has been further validated through agreement with PIH and the derivation of similar results through different physical principles and methods.

VII. ACKNOWLEDGMENTS

This work was supported by the Air Force Research Laboratory, Propulsion Directorate at Edwards AFB, CA.

[1] J. Slough, D. Kirtley, and T. Weber, Pulsed plasmoid propulsion: The elf thruster, in *31th International Electric Propulsion Conference*, 2009.

[2] A. J. Jamison, A. Ketsdever, and E. Muntz, Review of Scientific Instruments **73**, 3629 (2002).

[3] J. Lake, G. Cavallaro, G. Spanjers, P. Adkison, and M. Dulligan, in *Joint Propulsion Conference*, AIAA 2002-3821, 2002.

[4] M. Wilson, S. Bushman, and R. Burton, in *International Electric Propulsion Conference*, IEPC 97-122, 1997.

[5] M. Gamero-Castaño, V. Hruby, and M. Martinez-Sanchez, in *International Electric Propulsion Conference*, IEPC 01-235, 2001.

[6] H. Koizumi, K. Komurasaki, and Y. Arakawa, Review of Scientific Instruments **75**, 3185 (2004).

[7] J. K. Ziemer, Performance measurements using a submicronewton resolution thrust stand, in *International Electric Propulsion Conference*, number IEPC-01-238, 2001.

[8] N. Selden and A. Ketsdever, Review of Scientific Instruments **74**, 5249 (2003).

[9] B. D'Souza and A. Ketsdever, Review of Scientific Instruments **76**, 015105 (2005).

[10] A. P. Pancotti, *A Study of Ignition Effects on Thruster Performance of a Multi-electrode Capillary Discharge Using Visible Emision Spectroscopy Diagnostics*, PhD thesis, University of Southern California, 2009.

[11] N. Selden, N. Gimelshein, S. Gimelshein, and A. D. Ketsdever, Physics of Fluids **21**, 073101 (2009).

[12] R. H. Lee, A. M. Bauer, M. D. Killingsworth, T. C. Lilly, and J. A. Duncan, Performance characterization of the free molecule micro-resistojet utilizing water propellant, in *34th Joint Propulsion Conference*, AIAA 2007-5185, 2007.

[13] A. D. Ketsdever, R. H. Lee, and T. C. Lilly, Journal of Micromechanics and Microengineering **15**, 2254 (2005).

[14] B. D. D'Souza, A. D. Ketsdever, and E. P. Muntz, Investigation of transient forces produced by gases expelled from rapidly heated surfaces, in *24th International Symposium on Rarefied Gas Dynamics*, volume 762, pages 959–964, 2005.

[15] T. C. Lilly, S. F. Gimelshein, A. D. Ketsdever, and G. N. Markelov, Physics of Fluids **18** (2006).

[16] W. A. Johnson and L. K. Warne, Electrophysics of micromechanical comb actuators, in *Microelectromechanical Systems, Journal of*, volume 4, pages 49–59, 1995.